Average charge and its structure dependence of fragment ions under irradiation of a thin carbon foil with a 1-MeV/atom C_3^+ cluster ion

Atsuya Chiba,[1] Yuichi Saitoh,[1] Kazumasa Narumi,[2] Masahiro Adachi,[1] and Toshiaki Kaneko[3]
[1]*Takasaki Advanced Radiation Research Institute, Japan Atomic Energy Agency, Watanuki 1233, Takasaki, Gumma 370-1292, Japan*
[2]*Advanced Science Research Center, Japan Atomic Energy Agency, Watanuki 1233, Takasaki, Gumma 370-1292, Japan*
[3]*Department of Applied Physics, Okayama University of Science, Ridai-cho 1-1, Okayama 700-0005, Japan*
(Received 12 September 2006; revised manuscript received 10 August 2007; published 12 December 2007)

The charge states of fragment ions were measured for 1-MeV/atom C_3^+ cluster ions penetrating a carbon foil of 2.4-$\mu g/cm^2$ thickness. Those ions were detected by event-by-event mode with a fluorescent screen detector monitored by a charge-coupled device camera. The detected ion signals were traced by Coulomb explosion imaging technique, which enables us to classify charge states of each fragment ion and spatial arrangements of aligned cluster ions after emerging from the foil. Using this technique, we found the reduction of the average charge per ion. We also found that (i) the measured average charges of the aligned fragment ions in a linear-chain arrangement are larger than those in a triangular arrangement, and (ii) the edge-position ions in a linear-chain arrangement have the average charges greater than the middle-position ion. These experimental results are well supported by a recent refined theory on the cluster average charge.

DOI: 10.1103/PhysRevA.76.063201 PACS number(s): 36.40.Wa, 34.50.Fa, 39.10.+j

I. INTRODUCTION

Since swift polyatomic ions or clusters were available in accelerators, they have been intensively employed to investigate new information on ion-material interaction from viewpoints of both fundamental interest and potential application. Recent interest has been focused on highly charged biomolecules [1], fragmentation of clusters [2–5], breakup via Coulomb explosion [6], energy loss or energy deposition [7–10], and multiple ionization of clusters [11–13]. There, the number of atoms in a cluster ion and the spatial structure play a role of new characteristic parameters in collision-induced phenomena, while these never appear under single-ion irradiation. These two quantities together with projectile speed tend to control the interference effect, which stems from spatiotemporal correlation in collisions of a cluster ion with target electrons. Due to this effect, the resultant cluster-irradiation effect is not proportional to the number of atoms in a cluster. Indeed, this nonproportionality, which is called the vicinage effect, was observed in the energy loss [14,15] and the secondary electron emission yield [16–18].

The charge of an ion in a material is also important, because it determines the coupling strength of ion-target interaction [19–23]. So far, the fractional average charge Q/Z of a single ion with atomic number Z is well scaled as a function of the reduced ion speed to the average orbital speed $Z^{2/3}v_0(v_0=2.19\times10^8$ cm/s) [19,21]. Brunelle *et al.* [24], on the other hand, first reported the reduction of the average charge of the fragment ions under irradiation of carbon foils with MeV/atom C_n^+ $(n=3-10)$ ions. This reduction was enhanced with increasing the number of constituent atoms in a cluster, and with increasing the foil thickness, the reduction of the average charge of the fragment ions tends to vanish and approach the average charge of a single particle with the equivalent speed. This phenomenon was theoretically explained as the vicinage effect of the surrounding ions enhancing the binding energy of electrons in a considered ion [25]. The similar vicinage effect on the reduction of the average charge of the fragment ions was discussed by other researchers [26,27]. On the vicinage effect in the energy loss there is a pioneering work [28] and a nice review [29]. The reduction of the average charge of the fragment ions could be reconciled with the enhancement of the energy loss for MeV/atom cluster-ion incidence [25]. It was also predicted that the average charge depends on the structure of a cluster [25].

Carbon clusters are of special interest in that they have a number of spatial structures, i.e., linear chains, rings, cages, and fullerenes, with increasing the number of atoms [30,31]. This aspect provides us a widely ranging knowledge of correlation between spatial structure and reduction of the cluster average charge. Here, the cluster average charge is defined by the charge averaged over all constituent ions as

$$Q(n)=\left(\sum_{i=1}^{n}Q_i\right)\Big/n, \tag{1}$$

where Q_i and n denote, respectively, the charge state of the ith constituent ion and the number of the constituent ions in the cluster ion.

Vager and co-workers [32,33] reported a floppy linear structure for C_3^+ using Coulomb explosion imaging technique. Previously, we obtained the result, demonstrating that C_3^+ ions both in a linear-chain structure and in a triangular structure are included in the beam extracted from the tandem accelerator of JAEA/Takasaki [34]. This indicates that an incident C_3^+ ion could take various atomic arrangements due to the excitation in collision with a stripper gas in the accelerator. This variation of the atomic arrangement of C_3^+ enables us to study the relation between the structure and the average charge of fragment ions. In this paper, we report the cluster average charges measured by event-by-event technique under irradiation of a thin carbon foil with 1-MeV/atom C_3^+ cluster ions, and a part of them clearly showed the dependence on ion arrangement, and these are

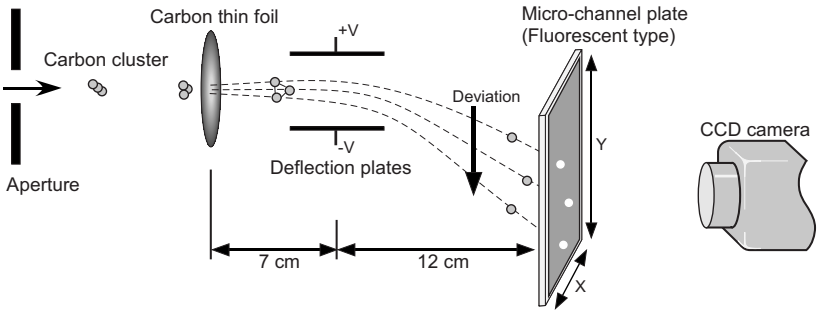

FIG. 1. Experimental setup.

compared with the calculated values predicted by a more refined theory.

II. EXPERIMENT

In this experiment, the charge averaging procedure defined by Eq. (1) was taken over only when three ions were detected on a fluorescent screen. In addition, we also picked up patterns of a linear chain or a triangle among them based on a structure classification by a trajectory calculation. Hereby we can obtain the dependence of the cluster average charge on ion arrangement. In a linear-chain arrangement, we determined the position-dependent average charge because we assigned the atomic positions of fragment ions just after emerging from a foil.

The experimental setup is schematically shown in Fig. 1. Carbon cluster ions (C_3^+) generated in a cesium sputter ion source were accelerated to 3 MeV (1 MeV/atom) by the tandem accelerator of JAEA/Takasaki. After the momentum analysis, the beam of C_3^+ ions was collimated by an *XY* slit and by an aperture to a diameter of 1 mm, and transported to a scattering chamber where the vacuum was in the range of 10^{-8} Torr. The intensity of incident C_3^+ ions was reduced at the rate of approximately 10–20 clusters per second both by a beam attenuator and by switching deflection plates, which were placed between the ion source and the accelerator. A self-supporting carbon foil of 2.4-$\mu g/cm^2$ thickness (ACF Metals) was used as the target. The transmitted ions were deflected depending on their charge states by an electric field applied to the horizontal deflection plates (the dimensions are 80 mm $\times$ 40 mm, the spacing between the plates is 30 mm, and the deflection voltage is $\pm$15 kV) placed between the foil and a microchannel plate (MCP). A two-dimensional pattern of the deflected ions was observed as luminance points on a fluorescent screen equipped with the MCP. The electrons emitted from the foil on the collision could not reach the MCP because of a negative potential of a few hundred volts applied to the first layer of the MCP. The pattern of luminance points on the screen was recorded with a charge-coupled device (CCD) camera as a digital image, which was stored in a personal computer, at 30 frames per second.

III. RESULTS AND DISCUSSION

A. Analysis of results

An example of the two-dimensional pattern of the transmitted ions is shown in Fig. 2(a) for 3-MeV C_3^+ ions incident on a carbon foil of 2.4 $\mu g/cm^2$ thickness. This figure corresponds to an accumulation of about 50 000 images recorded with the CCD camera. Figure 2(b) shows the charge-state distribution obtained by integrating the signals in Fig. 2(a) along the *x* axis. As obvious in the figure, the distribution has five peaks, which correspond to C^0 to C^{4+}, respectively. We have obtained 1.92 ± 0.01 as the cluster average charge defined by Eq. (1) from the charge-state distribution shown in Fig. 2(b), resulting in the reduction compared with the average charge of 2.02 ± 0.01 for the incidence of 1-MeV single C ions. The charge state of the constituent ions transmitting the carbon foil of 2.4 $\mu g/cm^2$ thickness is in equilibrium because the constituent atoms are positively ionized mainly in collisions with the target electrons at this energy, and the depth needed for the ion to attain the equilibrium charge state is about several nanometers [35]. This is also supported by the experimental data [24].

Next, in order to study the correlation between the average charge and the arrangement of the fragment ions which have just emerged from the foil, we picked up events which presented linear shapes and triangular shapes on the fluorescent screen. As it has been reported that C_3^+ can have a floppy linear structure [32,33], a C_3^+ projectile can be incident into the foil with various atomic arrangements. In the present study, we focused on a linear-chain arrangement and an equilateral-triangular arrangement, because they are two possible extreme atomic arrangements. Furthermore, we fo-

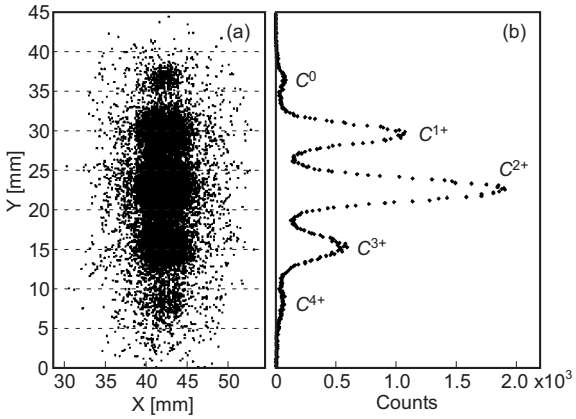

FIG. 2. (a) Accumulation of luminance points on the all imaging pictures recorded by the CCD camera, and (b) distribution of charge states obtained by integrating the accumulation along the *x* axis, measured on emerging from a 2.4-$\mu g/cm^2$ carbon foil, for a 1-MeV/atom C_3^+ projectile.

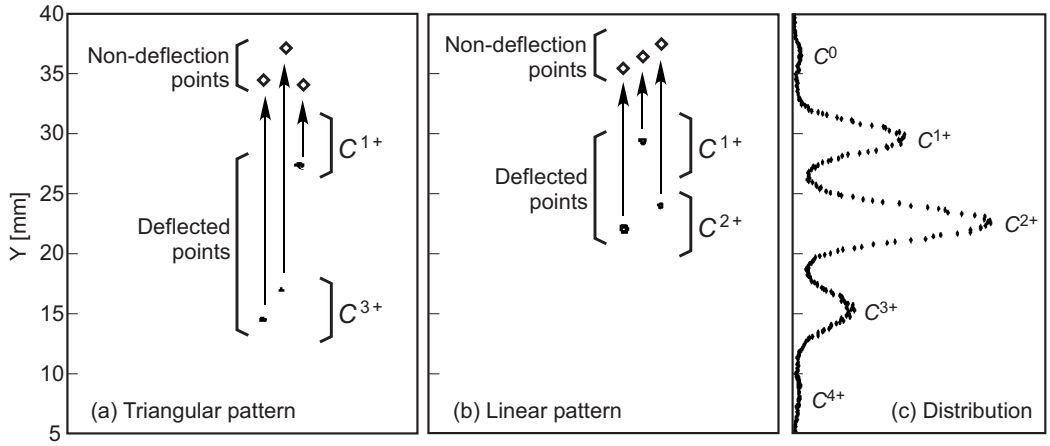

FIG. 3. Two patterns of the correlation of the deflected points and the nondeflection points. The charge state of each deflected point is identified by the relation between its position and charge distribution on the screen, described with (c). The instance of the pattern (a) becomes almost equilateral triangle, like the diamond symbols. The pattern (b) becomes the straight line at almost regular intervals, like the diamond symbols.

cused on C_3^+ projectiles which were incident into the foil with the plane including three constituents of the cluster or the cluster chain almost perpendicular to the incident direction. In such a case, the influence of wake force, which affects the relative motion among the fragment ions in the foil, is smallest. Therefore the atomic arrangement of fragment ions which have just exited from the foil reflects the initial arrangement of an incident C_3^+ most directly even if other influence such as multiple scattering, energy loss and struggling, and so on are considered. Thus this enables us to deduce the arrangement of the fragment ions just after the foil from the two-dimensional pattern of the detected transmitted ions on the fluorescent screen by the Coulomb explosion imaging technique. Based on the trajectory calculation considering the Coulomb explosion and the multiple scattering, we have classified the arrangement of the fragment ions just after the foil into the linear-chain arrangement and the triangular arrangement as follows: At first, we derived the fragment-ion distribution which was observed on the fluorescent screen without the deflection for the charge-state measurement; hereafter, we will call this distribution the nondeflection points. The nondeflection points can be derived from the present observed pattern, which we call the deflected points, with the deflection for the charge-state measurement, because the charge state of each transmitted ion can be known by its position on the screen. Figure 3 shows instances of how we have derived the nondeflection points from the deflected points. Next, we plotted all of the detected nondeflection points in the following symmetric coordinates:

$$S_2 = (D_{12} - D_{23})/\sqrt{2},$$

$$S_3 = (2D_{31} - D_{23} - D_{12})/\sqrt{6},$$

$$D_{ij} = d_i/d_j,$$

where d_i is the distance from the center of gravity of the pattern to the nondeflection point i. All possible permutations of i and j are included. In these coordinates, the origin ($S_2 = S_3 = 0$) corresponds to an equilateral-triangle pattern ($D_{12} = D_{23} = D_{31}$); the larger the deviation of the nondeflection points from the equilateral triangle, the larger the distance from the origin; in the case of a linear pattern at exact regular intervals, S_2 and S_3 diverge. Figure 4 shows all of the detected nondeflection points in the (S_2, S_3) symmetric coordinates. Finally, we classified the distribution of the nondeflection points in triangular and linear-chain patterns following the criterion described below: We defined nondeflection points in the domain enclosed with a solid line near the origin in Fig. 4 as the triangular pattern and those in the three symmetric domains enclosed with a broken line as the linear-chain pattern. This definition is based on the trajectory calculation that included the Coulomb explosion and the mul-

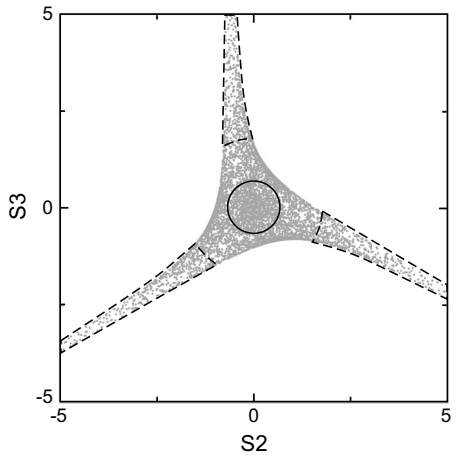

FIG. 4. The plots for all of the nondeflection points in the symmetric coordinates for the structure classification (see text). The contour domains which were estimated by a trajectory calculation represent each cluster structure in the condition that the plane of the incident cluster-ion is parallel to a foil. The triangular structure occupies 70% in the central domain enclosed with a solid line; the abundance ratio of the linear-chain structure in the three symmetric domains enclosed with a broken line is 90%.

TABLE I. Average charges of fragment ions for the 1-MeV/atom C_3^+ cluster ion, penetrating a carbon foil of 2.4-$\mu g/cm^2$ thickness: (a) structure dependence and (b) atomic-position dependence in a linear-chain arrangement.

(a)	Linear	Triangular	(b)	Center	Edge
Expt.	1.96±0.03	1.89±0.02	Expt.	1.86±0.04	2.01±0.03
Calc.	1.91	1.89	Calc.	1.88	1.93

tiple scattering in condition that the cluster plane was exiting from a foil in parallel. The calculation shows that most of the triangular patterns of all combinations from C^+ to C^{4+} belong to the domain enclosed with a solid line; on the other hand, the three symmetric domains enclosed with a broken line are almost occupied by the linear-chain patterns. The nondeflection points in Fig. 3(a) cited as the instances belongs to the central domain enclosed with a solid line in the symmetric coordinate, and the pattern in Fig. 3(b) belongs to the three symmetric domains enclosed with a broken line. Following this criterion, we extracted the applicable images from all of the observed images, and analyzed approximately 400 images for each pattern. Hereby the cluster average charge for the triangular pattern and the linear-chain pattern was obtained.

As summarized in Table I(a), the cluster average charge obtained for the linear pattern is larger than that for the triangular pattern. This result indicates that the cluster average charge depends on the arrangement of the fragment ions just after the foil. Moreover, we have evaluated the position-dependent average charge of the transmitted ions belonging to the linear pattern, which shows that the average charge of the two edge-position ions is larger than that of the middle-position ion as shown in Table I(b). The difference between the average charge of the two edge-position ions and that of the middle-position ion indicates that the incident C_3^+ ions resulting in the linear pattern on the detection plate do not have a triangular arrangement but have a linear-chain arrangement. There is a possibility that the incident C_3^+ ion in a triangular arrangement happens to show a linear pattern on the fluorescent screen and vice versa. In order to check our classification, we carried out Monte Carlo simulation, by taking into account multiple scattering, for the triangular and linear-chain arrangements of clusters emerging from the foil in various charge-state combinations. According to our simulation, the fraction of a linear-chain arrangement resulting in a triangular pattern on the detection plate was estimated to be 20% at most in cases of the three-C^{2+} pattern. On the contrary, it is very rare that a triangular arrangement results in a linear-chain pattern on the plate. In addition, our experimental data show that the average charge of linear patterns yielded larger than that of triangular ones. Therefore if the contribution of the linear-chain arrangements to the triangular patterns could be excluded, the difference in the average charge of clusters in the linear and triangular patterns would be a little enhanced, rather than what the present data indicate.

B. Comparison with the theoretical average charge

In order to compare the experimental data, the average charges of constituent ions of the cluster were calculated on the basis of a refined version of Refs. [25,36]. A self-consistent average-charge theory for swift cluster ions in solids was presented [25]. Refinement of the theory was made through taking into account a repulsive Coulomb force (not a pointlike force), the polarization force (i.e., the slowing-down force and the wake force) in the dielectric media, and the elastic scattering between a constituent ion with a target atom in a small-angle multiple scattering approximation [37–39]. In this calculation, we treated each ion as a partially stripped ion with the average charge, determined self-consistently [25], and with the corresponding average number of bound electrons. The average charge of isolated ions with the equivalent speed in this media is about 2 and the outer electrons will be stripped off, so that we are allowed to treat the cluster as an ensemble of isolated ions with the nearest-neighbor distance setting to be $2.4a_0$ ($a_0=0.53\times10^{-8}$ cm) both in the linear-chain and in the triangular arrangements. The time evolution of the interatomic separations due to Coulomb explosion and the polarization force is estimated by means of a molecular dynamics (MD) simulation. Let us denote the cluster speed and the charge of the jth ion in the Fourier space, respectively, by v and $\rho_j(\vec{k})$. Then the polarization force (including the slowing-down and the wake) acting on the jth ion in a solid is described in the dielectric-function form as follows:

$$\vec{F}_{j_\perp} = \frac{2}{pv}\int_0^\infty dk_\perp k_\perp^2 \int_0^\infty d\omega \rho_j(\vec{k}) \sum_i \rho_i(\vec{k}) \frac{J_1(k_\perp R_{ji\perp})}{k_\perp^2 + (\omega/v)^2} \vec{n}_{ji\perp} \times \left[\cos\left(\frac{\omega}{v} R_{jiz}\right) \mathrm{Re}\left\{ \frac{1}{\varepsilon(k,\omega)} - 1 \right\} - \sin\left(\frac{\omega}{v} R_{jiz}\right) \mathrm{Im}\left\{ \frac{1}{\varepsilon(k,\omega)} - 1 \right\} \right],$$

$$\vec{F}_{j_z} = \frac{2}{\pi v^2}\int_0^\infty dk_\perp k_\perp \int_0^\infty d\omega \omega \rho_j(\vec{k}) \sum_i \rho_i(\vec{k}) \frac{J_0(k_\perp R_{ji\perp})}{k_\perp^2 + (\omega/v)^2} \vec{n}_{jiz} \times \left[\cos\left(\frac{\omega}{v} R_{jiz}\right) \mathrm{Im}\left\{ \frac{1}{\varepsilon(k,\omega)} \right\} + \sin\left(\frac{\omega}{v} R_{jiz}\right) \times \mathrm{Re}\left\{ \frac{1}{\varepsilon(k,\omega)} - 1 \right\} \right],$$

with $k^2=k_\perp^2+(\omega/v)^2$. Here $\varepsilon(k,\omega)$ is the dielectric function of the carbon [25]. In addition to the above force, the pure Coulomb forces also act on the individual partially stripped ions. The charge $\rho_j(\vec{k})$ is given by atomic number Z_j and the form factor $\rho_{je}(k)$ in the Thomas-Fermi-Moliere form [25], as $\rho_j(k)=\{Z_j-\rho_{je}(k)\}e$, where $\rho_{je}(k)$ includes the average

number of the bound electrons, determined self-consistently by the ion speed, the charges of surrounding ions, and the distances from them. $J_n(k_{ji\perp}R_{ji\perp})$ $(n=0,1)$ is the nth order Bessel function of the first kind. The subscripts z and $\perp$ denote the direction of the incident ion beam and the direction perpendicular to the z direction, respectively. The unit vectors $\vec{n}_{jiz}$ and $\vec{n}_{ji\perp}$ denote the corresponding components of the relative position vector $\vec{R}_{ji}$ of the jth and ith ions. Re$\{a\}$ and Im$\{a\}$ are the real part and the imaginary part of the complex number a, respectively.

Calculation was performed for the perpendicular arrangement for incidence of the linear-chain and the triangular C_3 clusters. The calculated average charges of fragment ions just emerging from the foil are shown in Table I. Here the average charges of the constituent ions were assumed to be unchanged once they emerge from the foil. For a C_3 cluster in the triangular arrangement, the average charge of three fragment ions is 1.89. On the other hand, in the linear-chain C_3 cluster the average charge of constituent ions is 1.91, and the average charge of the edge-position ions and that of the middle-position ion are, respectively, 1.93 and 1.88. This is due to that the middle-position ion is affected from both sides by the field of two edge-position ions, resulting in having the lowest average charge among them. It is found that this tendency was not changed by the wake force. These results are at least qualitatively consistent with the experimental data. Here we treat elastic scattering as a small-angle multiple scattering with screening lengths [36,39] since large-angle elastic scattering events prevent us from detecting three ions on the screen. This effect on the average charges is negligibly small because of a thin foil. The order in which ions leave the rear surface of the foil is also taken into account. For aligned arrangements of emergent ions (almost perpendicular to the incident direction), this ordering effect is very small since there is little time difference in emerging from the foil.

IV. CONCLUSION

We measured by event-by-event technique the cluster average charge of 1-MeV/atom C_3^+ cluster emerging from a carbon foil of 2.4 $\mu g/cm^2$, which is 1.92 ± 0.01. For atomic arrangements where the cluster plane is almost perpendicular to the incident direction, the average charge in the linear-chain arrangement is a little larger than in the triangular one. In the former case, the edge-position ions have a larger average charge than the middle-position ion. The conclusion obtained using this foil thickness is not a special one but a rather general one, since the charge state can attain the equilibrium state and the reduction in the cluster average charge can be also obtained except in very thin foils where the charge state will be in a pre-equilibrium state (probably less than 1 $\mu g/cm^2$ for 1-meV/atom C_3^+ cluster incidence). The present event-by-event mode technique has the potential to clarify the correlation between the average charge of the constituent ions and the spatial structure of them in an aligned arrangement in more complex cluster-ion impacts.

ACKNOWLEDGMENTS

The authors are grateful to the crew of the 3-MV Tandem accelerator of JAEA/Takasaki. One of the authors (T.K.) would like to acknowledge support of the academic frontier project at OUS by MEXT, and a Grant-in-aid for Scientific Research (C) from JSPS.

[1] P. Attal, S. Della-Negra, D. Gardes, J. D. Larson, Y. Le Beyec, R. Vienet-Legue, and B. Waast, Nucl. Instrum. Methods Phys. Res. A **328**, 293 (1993).
[2] B. Farizon, M. Farizon, M. J. Gaillard, E. Gerlic, and S. Ouaskit, Nucl. Instrum. Methods Phys. Res. B **88**, 86 (1994).
[3] A. Itoh, H. Tsuchida, T. Majima, and N. Imanishi, Phys. Rev. A **59**, 4428 (1999).
[4] H. Tsuchida, A. Itoh, K. Miyabe, Y. Bitoh, and N. Imanishi, J. Phys. B **32**, 5289 (1999).
[5] T. LeBrun, H. G. Berry, S. Cheng, R. W. Dunford, H. Esbensen, D. S. Gemmell, E. P. Kanter, and W. Bauer, Phys. Rev. Lett. **72**, 3965 (1994).
[6] A. Faibis, G. Goldring, M. Hass, R. Kaim, I. Plesser, and Z. Vager, Nucl. Instrum. Methods Phys. Res. **194**, 299 (1982).
[7] M. Vicanek, I. Abril, N. R. Arista, and A. Gras-Marti, Phys. Rev. A **46**, 5745 (1992).
[8] A. Brunelle, S. Della-Negra, J. Depauw, D. Jacquet, Y. Le Beyec, M. Pautrat, and Ch. Schoppmann, Nucl. Instrum. Methods Phys. Res. B **125**, 207 (1997).
[9] T. Kaneko, Nucl. Instrum. Methods Phys. Res. B **153**, 15 (1999).
[10] E. Ray, R. Kirsch, H. H. Mikkelsen, J. C. Poizat, and J. Remillieux, Nucl. Instrum. Methods Phys. Res. B **69**, 133 (1992).
[11] K. Wohrer, M. Chabot, J. P. Rozet, D. Gardes, D. Vernhet, D. Jacquet, S. Della-Negra, A. Brunelle, M. Nectoux, M. Pautrat, Y. Le Beyec, P. Attal, and G. Maynard, J. Phys. B **29**, L755 (1996); M. Chabot, K. Whorer, J. P. Rozet, D. Gardes, D. Vernhet, D. Jacquet, S. Della-Negra, A. Brunelle, M. Nectoux, M. Pautrat, and Y. Le Beyec, Phys. Scr. **T73**, 282 (1997).
[12] H. Tsuchida, A. Itoh, Y. Nakai, K. Miyabe, and N. Imanishi, J. Phys. B **31**, 5383 (1998).
[13] T. Wada and T. Kaneko, J. Phys. Soc. Jpn. **74**, 918 (2005).
[14] K. Narumi, K. Nakajima, K. Kimura, M. Mannami, Y. Saitoh, S. Yamamoto, Y. Aoki, and H. Naramoto, Nucl. Instrum. Methods Phys. Res. B **135**, 77 (1998).
[15] K. Baudin, A. Brunelle, M. Chabot, S. Della-Negra, J. Depauw, D. Gardes, P. Hakansson, Y. Le Beyec, A. Bellebaud, M. Fallavier, J. Remillieux, J. C. Poizat, and J. P. Thomas, Nucl. Instrum. Methods Phys. Res. B **94**, 341 (1994).
[16] H. Kudo, W. Iwazaki, R. Uchiyama, S. Tomita, K. Shima, K. Sasa, S. Ishii, K. Narumi, H. Naramoto, Y. Saitoh, S. Yamamoto, and T. Kaneko, Jpn. J. Appl. Phys., Part 2 **45**, L565 (2006).
[17] S. Tomita, S. Yoda, R. Uchiyama, S. Ishii, K. Sasa, T. Kaneko, and H. Kudo, Phys. Rev. A **73**, 060901(R) (2006).
[18] T. Kaneko, H. Kudo, S. Tomita, and R. Uchiyama, J. Phys.

Soc. Jpn. **75**, 034717 (2006).
[19] N. Bohr, K. Dan. Vidensk. Selsk. Mat. Fys. Medd. **18**, No. 8 (1948).
[20] I. S. Dmitriev and V. S. Nikolaev, Zh. Eksp. Teor. Fiz. **47**, 615 (1964) [Sov. Phys. JETP **20**, 409 (1965)].
[21] H. D. Betz, G. Hortig, E. Leischner, Ch. Schmelzer, B. Stadler, and J. Weihrauch, Phys. Lett. **22**, 643 (1966).
[22] A. B. Wittkower and H. D. Betz, At. Data **5**, 113 (1973).
[23] K. Shima, T. Mikumo, and H. Tawara, At. Data Nucl. Data Tables **34**, 357 (1986).
[24] A. Brunelle, S. Della-Negra, J. Depauw, D. Jacquet, Y. Le Beyec, and M. Pautrat, Phys. Rev. A **59**, 4456 (1999).
[25] T. Kaneko, Phys. Rev. A **66**, 052901 (2002).
[26] Z. L. Miskovic, S. G. Davison, F. O. Goodman, W. K. Liu, and Y. N. Wang, Phys. Rev. A **61**, 062901 (2000).
[27] S. Heredia-Avalos, R. Garcia-Molina, and N. R. Arista, Europhys. Lett. **54**, 729 (2001).
[28] W. Brandt, A. Ratkowski, and R. H. Ritchie, Phys. Rev. Lett. **33**, 1325 (1974).
[29] N. R. Arista, Nucl. Instrum. Methods Phys. Res. B **164-165**, 108 (2000).
[30] W. Weltner, Jr. and R. J. VanZee, Chem. Rev. (Washington, D.C.) **89**, 1713 (1989).
[31] G. D. Carney and R. N. Porter, J. Chem. Phys. **65**, 3547 (1976); A. V. Orden and R. J. Saykally, Chem. Rev. (Washington, D.C.) **98**, 2313 (1998).
[32] Z. Vager, R. Naaman, and E. P. Kanter, Science **244**, 426 (1989).
[33] Z. Vager and E. P. Kanter, J. Phys. Chem. **93**, 7745 (1989).
[34] A. Chiba, Y. Saitoh, and S. Tajima, Nucl. Instrum. Methods Phys. Res. B **232**, 32 (2005).
[35] T. Kaneko and Y. H. Ohtsuki, Phys. Status Solidi B **111**, 491 (1982).
[36] T. Kaneko and S. Ikegami, Nucl. Instrum. Methods Phys. Res. B **258**, 57 (2007).
[37] J. Lindhard, V. Nielsen, and M. Scharff, K. Dan. Vidensk. Selsk. Mat. Fys. Medd. **36**, No. 10 (1968).
[38] P. Sigmund and K. B. Winterbon, Nucl. Instrum. Methods **119**, 541 (1974).
[39] S. Ikegami and T. Kaneko, Bull. Okayama Univ. Sci. **42**A, 21 (2006).